OCEANOGRAPHY

Pulses of South Atlantic water into the tropical North Atlantic since 1825 from coral isotopes

Martine Paterne[1]*, Ellen R. M. Druffel[2], Thomas P. Guilderson[3], Dominique Blamart[1], Christophe Moreau[4], Jennifer Weil-Accardo[5], Nathalie Feuillet[6]

Decadal and multidecadal changes in the meridional overturning circulation may originate from either the subpolar North Atlantic or the Southern Hemisphere. New records of carbon and oxygen isotopes from an eastern Martinique Island (Lesser Antilles) coral reveal irregular, decadal, double-step events of low $\Delta^{14}C$ and enhanced vertical mixing, high $\delta^{18}O$ and high $\delta^{13}C$ values starting in 1885. Comparison of the new and published $\Delta^{14}C$ records indicates that the last event (1956–1969) coincides with a widespread, double-step $\Delta^{14}C$ low of South Atlantic origin from 32°N to 18°S, associated with a major slowdown of the Caribbean Current transport between 1963 and 1969. This event and the past Martinique $\Delta^{14}C$ lows are attributed to pulses of northward advection of low $\Delta^{14}C$ Sub-Antarctic Mode Waters into the tropical Atlantic. They are coeval with changes of the tropical freshwater budget and likely driven by meridional overturning circulation changes since ~1880.

INTRODUCTION

The Atlantic meridional overturning circulation (MOC) connects the Pacific and Indian Oceans to the Atlantic Ocean through an upper, northward flow of warm salty water and a deeper, southward flow of cold and fresher North Atlantic deep water. Thereby, it plays a major role in controlling northward heat transport and climate in the North Atlantic region and heat and carbon storages to the deep ocean [e.g., (*1*, *2*)]. Observations and modeling studies of MOC variability predominantly focus on the subpolar and subtropical North Atlantic regions and on the hydrographic and atmospheric mechanisms affecting deep water formation in the subpolar North Atlantic at the decadal and multidecadal timescales [e.g., (*1*–*3*)]. Recent studies have highlighted the role of gyre-specific dynamics on MOC (*3*–*6*), notably that of the South Atlantic subtropical gyre linked to anomalous subsurface leakages from the Pacific and Indian Oceans (*4*–*6*). While little is known about the southern-induced MOC changes due to the lack of long-term observations, these changes may deeply affect the subtropical North Atlantic heat content and oceanic circulation (*4*, *5*), and influence hurricane frequency and rainfall patterns [e.g., (*2*)].

The Caribbean Current (CC), a precursor of the Florida Current and the Gulf Stream (GS), is a pathway of the interhemispheric upper flow of the MOC (Fig. 1). It is composed of approximately equal to North and South Atlantic inflows into the Caribbean Sea (*7*, *8*). These are formed by an upper (~100 m) flow and a lower one (>300 m) of South Atlantic origin, bounding the Central Waters of mainly North Atlantic origin (*7*). The North Atlantic water (NAW) is transported southwestward by the return flow of the GS along the North Atlantic subtropical gyre that feeds the westward flows of the Antilles Current (AC) and of the North Equatorial Current (NEC) (*9*). The North Brazil Current (NBC), fed by the westward flow of the South Equatorial Current (SEC), advects the South Atlantic water (SAW) northward into the Caribbean Sea and along the eastern Lesser Antilles in the form of NBC rings (*9*). On its path, it entrains the freshwater plumes of the world's two largest rivers, the Amazon and Orinoco into the eastern Caribbean Sea (*10*) and the western tropical North Atlantic (*11*).

Tropical salinity anomalies play a major role in the decadal and multidecadal variability of the global current strengths and on MOC changes (*12*, *13*). As an example, model-based experiments of oceanic circulation without Amazon runoff show stronger global currents and a ~10-year later strengthening of MOC due to the spread of the tropical salinity–induced anomaly into the northern North Atlantic sites of deep water formation (*13*). MOC strengthening leads to an anomalous northward migration of the tropical rainfall belt of the Intertropical Convergence Zone and to major droughts over the Amazonian basin (*13*). Documenting the long-term hydrographic and transport changes of the CC is important to gain knowledge on natural climate variability and model prediction of climate change.

Here, we report the annual time-series measurements of $\Delta^{14}C$ and the stable isotopes of carbon and oxygen between 1825 and 2006 from an annually banded coral, *Siderastrea siderea*, cored alive on the Atlantic coast of Martinique Island (14°70 N, 60°90 W in 1.50-m water depth) in the tropical North Atlantic (table S1) (*14*). Radiocarbon (^{14}C) in corals records the same $^{14}C/^{12}C$ ratio of the dissolved inorganic carbon (DIC) in seawater in which corals grow, providing a powerful tracer of past, mean ocean circulation. It is expressed as Δ [per mil (‰)], the deviation in parts per thousand (ppt) of a sample's $^{14}C/^{12}C$ ratio corrected for year of growth from that of the absolute standard activity in 1950 (*15*). The $\delta^{18}O$ of the coral skeleton reflects the sea surface temperature (SST) and seawater $\delta^{18}O$ ($\delta^{18}O_{sw}$) at the time of formation (*16*). $\delta^{18}O_{sw}$ values are related to sea surface salinity (SSS), linked to the freshwater budget {evaporation (E) − [precipitation (P) + runoff (R) budget]}. The skeletal $\delta^{13}C$ values of hermatypic corals are controlled by biological processes and change in surface DIC

[1]Laboratoire des Sciences du Climat et de l'Environnement, LSCE/IPSL, CEA-CNRS-UVSQ, Université Paris-Saclay, Domaine du CNRS, F-91198 Gif-sur-Yvette, France. [2]Department of Earth System Science, University of California, Irvine, Irvine, CA 92697-3100, USA. [3]Ocean Sciences Department, University of California, Santa Cruz, Santa Cruz, CA 95604 USA. [4]LMC14, UMS 2572, CEA/Saclay, Bâtiment 450, porte 4E, 91191 Gif-sur-Yvette Cedex, France. [5]Aix Marseille University, CNRS, IRD, INRAE, CEREGE, Aix-en-Provence, France. [6]Institut de Physique du Globe de Paris, UMR 7154, CNRS Paris Sorbonne Paris Cité, Paris, France.
*Corresponding author. Email: martine.paterne@lsce.ipsl.fr

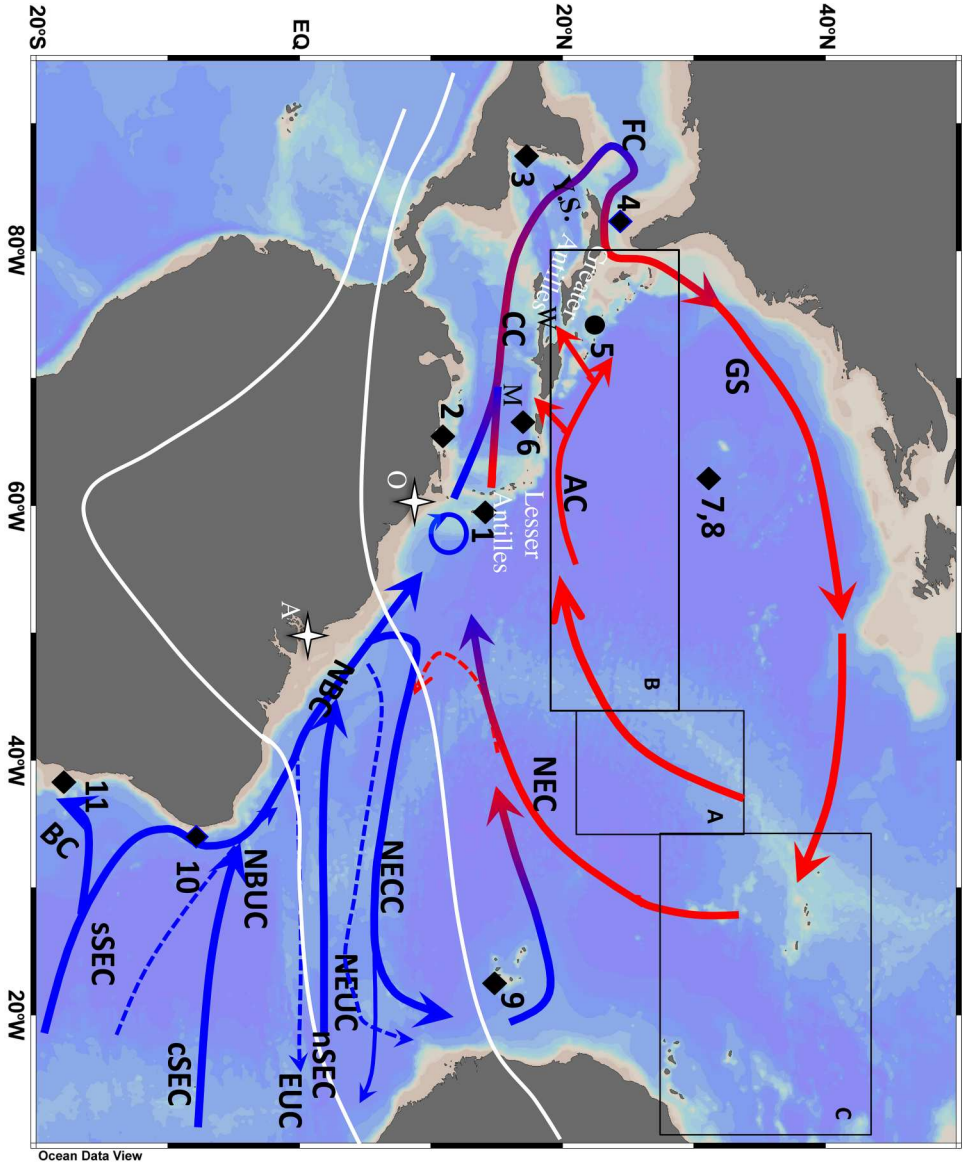

Fig. 1. Location of coral (diamond) and scleroponge (circle) samples used in this study and schematic view of the tropical and subtropical Atlantic currents. They are reported on ocean data view map (*46*). (1) Martinique: 14°70 N, 60°90 W in 1.50-m water depth (table S1); (2) Cariaco basin (Bocca di Medio) (*19*–*21*); (3) Belize coral (*22*); (4) Florida Pickle Reef (*22*–*24*, *38*); (5) Bahamas (*25*); (6) Puerto Rico (*26*); (7) Bermuda North shore (*27*–*29*); (8) Bermuda South shore (*30*); (9) Cape Verde (*25*, *28*); (10) Punta Galinha (*28*); (11) Abrolhos (*28*). Yucatan Strait is noted Y.S., and river mouths of Amazon (A) and Orinoco (O) are denoted by white stars. Schematic current transports of NAW (red), SAW (blue), and mixed NAW and SAW (mixed colored) waters are represented at sea surface and thermocline depth by bold and dashed lines, respectively (*44*). NBUC, North Brazil Undercurrent; NECC, North Equatorial Countercurrent; NEUC, North Equatorial Undercurrent; EUC, Equatorial Undercurrent; nSEC, cSEC, and sSEC, north, central, and South Equatorial currents. W and M are the Windward and the Mona passages through the Greater Antilles. White lines refer to the approximate northern summer and southern winter locations of the Intertropical Convergence Zone. Boxes A to C indicate the areas of post-1950 time series of sea surface measurements of $\Delta^{14}C$ (table S2).

$\delta^{13}C$ linked to air-sea CO_2 exchange and environmental factors (*17*).

The Martinique coral is located in the transition region from a southern NBC transport of SAW and of Amazon river and Orinoco river fresh waters to a northern NEC transport of NAW (*18*), permitting the investigation of past tropical Atlantic changes. The Martinique record of $\Delta^{14}C$ is compared to published records from intra– and extra–Caribbean Sea corals (*19*–*30*) and a scleroponge (*25*), all precisely dated either by sclerochronology (*19*–*24*, *26*–*30*) or by Th/U dating (*25*) (Fig. 1, figs. S1 to S4, and table S2). These records allow the annual reconstruction of mixing proportions of NAW and SAW within the CC beyond the well-detailed post-1950 time interval.

RESULTS

The oxygen and carbon isotope results have been obtained on the same annual samples of the Martinique coral (Fig. 2 and table S1)

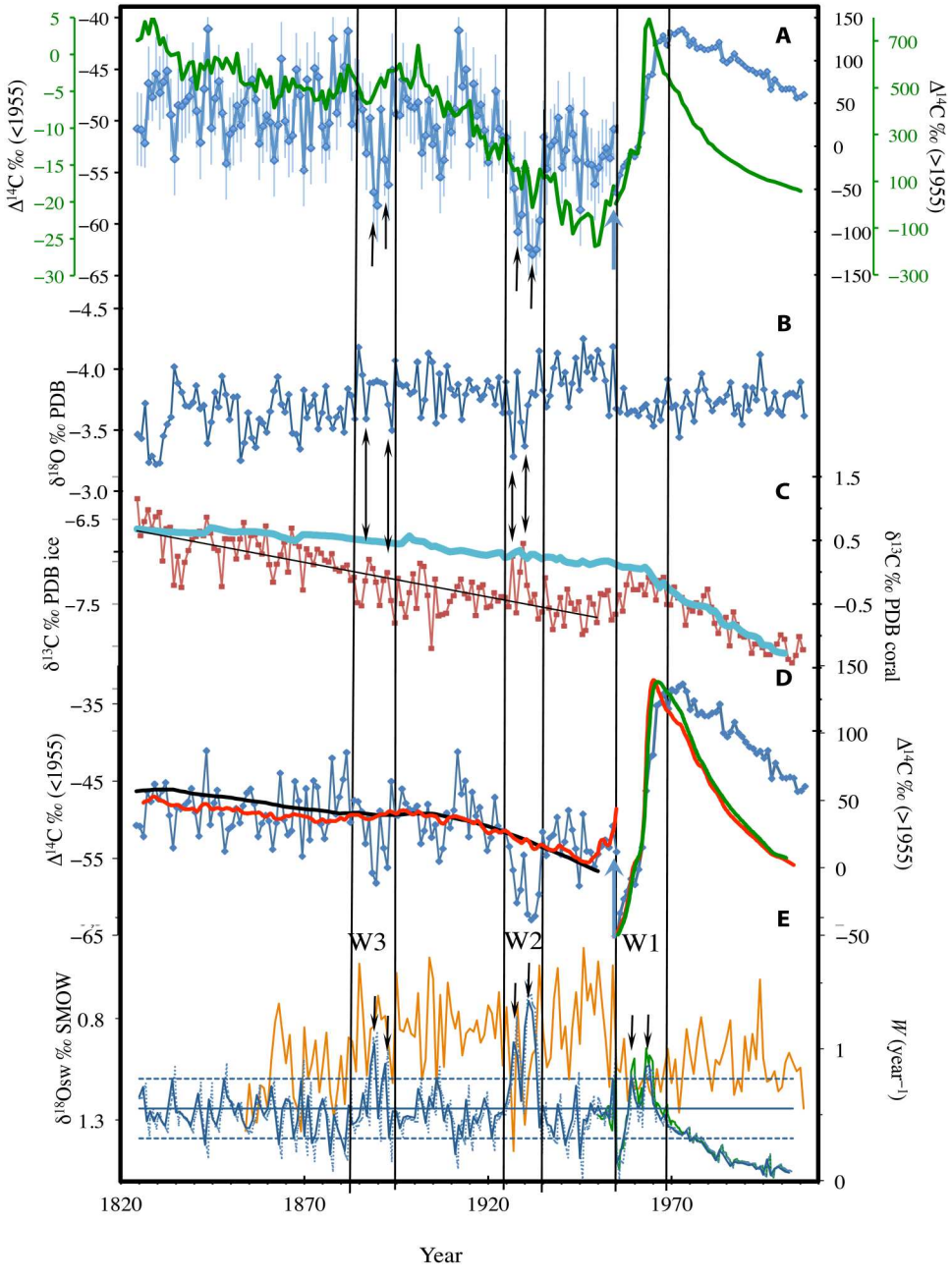

Fig. 2. Variations of carbon and oxygen isotopes and vertical mixing *W* as a function of time (year) in the Martinique coral bands. Records of (**A**) $\Delta^{14}C$ (‰) and uncertainties (1σ) (blue diamonds) and of the atmosphere (green line) from the single-year IntCal98 (*36*) and NHZone 2 (*31*) records in the pre- and post-1955 time interval. Note the change in the *y* axes for the prebomb $\Delta^{14}C$ (left axis) and postbomb $\Delta^{14}C$ (right axis) records. (**B**) $\delta^{18}O$ [‰, Pee Dee Belemnite (PDB)] (blue diamonds) and (**C**) $\delta^{13}C$ (‰, PDB) in Antarctic firn (*35*) (cyan line; left axis) and in Martinique coral (red squares; right axis). The black line represents the least squares fit with regression of −0.011‰/year before 1950, (**D**) pre-1950 (left axis), and post-1950 (right axis) Martinique $\Delta^{14}C$ (‰) (blue diamonds) and steady-state values of $\Delta^{14}C$ (black line) using Druffel's box model (*29*) using the NEC values from Bermuda $\Delta^{14}C$ (*27*–*30*) (red) and from sea surface $\Delta^{14}C$ of the southern subtropical Atlantic (green) (box C in Fig. 1 and table S1). The bold black line is the modeled marine global curve IntCal98 (*36*). (**E**) Sea surface water $\delta^{18}O$ [$\delta^{18}O_{sw}$; ‰, standard mean ocean value (SMOW)] (yellow lines; left axis) and vertical mixing *W* (right axis) using the inverse box model (*29*) in year^{-1} using the Bermuda $\Delta^{14}C$ (*27*–*30*) (thin blue line represents changes at the 0.2-year step, and bold dashed blue line represents the annual changes) and using sea surface $\Delta^{14}C$ of the southern subtropical Atlantic (green) (box C in Fig. 1 and table S2). Thin bold and dashed blue lines represent the mean values and variance of *W* at 2SD between 1825 and 1835. The vertical black lines and the black arrows represent the age limits and the double-step structure of W1, W2, and W3, respectively. The blue arrows indicate the change of the $\Delta^{14}C$ scale in 1955.

(see Materials and Methods). The $\Delta^{14}C$ values range from −41 to −63‰ in the pre-1955 growth bands with uncertainties at 1σ of ±3.5‰ (Fig. 2A; fig. S1, A and B; and table S1). Significant decadal $\Delta^{14}C$ decreases of ~10 to 15‰ occur, with a double-peak structure, between 1885 and 1895 and between 1925 and 1935. The double peaks of low $\Delta^{14}C$ between 1901 and 1909 are of smaller amplitude (7‰). In the post-1955 bands, the $\Delta^{14}C$ values increase in 1956 due to the atmospheric bomb ^{14}C rise (*31*) and reach a plateau in 1959–1960. Then, values increase from −12 to 80‰ (1961 and 1964) until another plateau is reached in 1964–1965. Surface water (coral) $\Delta^{14}C$ greatly increase in 1966 (84 to 120‰) and then moderately (120 to 136‰) peaking in 1973, while atmospheric values decrease. Then, the coral $\Delta^{14}C$ decreases by ~75‰ over the past 33 years along rapid steps of ~10‰ every 6 to 10 years.

Values of $\delta^{18}O$ range between −3.17 and −4.25‰ and exhibit 0.3 to 0.5 ‰ interannual and decadal fluctuations (Fig. 2B and table S1). A major increase of 0.55‰ occurs between 1954 and 1958. The values of $\delta^{18}O_{sw}$ decrease from 1.3‰ in the mid-1850s to 0.9‰ in the early 1880s (Fig. 2E and figs. S5 and S6). Then, values vary by 0.4‰ around the mean value of 0.85‰ between 1880 and 1955 and by 0.12‰ around the mean of 1.0‰ between 1969 and 2006, close to the modern sea surface value (*32*). These variations amount to ~2 and ~1 ppt of SSS, respectively, consistent with the reported interannual variations of SSS in the western tropical North Atlantic (*33*). Between 1954 and 1968, the values of $\delta^{18}O_{sw}$ increase by 0.6‰, representing an increase in SSS of 2.6 ppt.

The values of $\delta^{13}C$ exhibit the long-term decrease in corals and scleroponges, commonly known as the ^{13}C Suess effect (Fig. 2C and table S1) (*17*, *34*). They, however, show a significant increase of 0.025‰/year (r^2 = 0.34) between 1950 and 1969. It separates a first decreasing trend of −0.011‰/year between 1825 and ~1950 (r^2 = 0.64) from a second one of greater amplitude of −0.026‰/year (r^2 = 0.73) between 1969 and 2006 (Fig. 2C). The first trend includes a sharp increase of ~0.9‰ between 1925 and 1935 and high variability of ~0.6 to 0.7‰ between 1885 and 1910. In summary, the prominent, decadal $\Delta^{14}C$ decreases of ~10 to 15‰ between 1925 and 1935 and between 1885 and 1895 are coeval with double-step increases in $\delta^{18}O_{sw}$ and $\delta^{18}O$ and $\delta^{13}C$ in the pre-1950 coral bands (Fig. 2).

DISCUSSION

Between 1825 and 1950, the annual changes of $\delta^{13}C$ and $\Delta^{14}C$ in the Martinique coral record are mainly controlled by ocean processes, rather than by air-sea CO_2 exchange. The decrease in coral $\delta^{13}C$ values is about three times greater than that in the atmosphere (Fig. 2C) (*35*). The Martinique coral $\Delta^{14}C$ has recorded a Suess effect of small amplitude of −4.7‰ (±1.3‰), using the weighted mean and error values in the pre-1850 (−48.7‰) and post-1940 (−53.5‰) coral bands. Only 25% of the long-term changes of the Martinique coral $\Delta^{14}C$ are linearly correlated with atmospheric fluctuations of $\Delta^{14}C$ (*36*) as shown by the regression coefficients with either a 0-year time lag (r^2 = 0.27) or a 12-year time lag (r^2 = 0.25), the latter matching the timing of isotopic equilibration for ^{14}C in the mixed layer (*37*). The correlations are tied to the decrease in $\Delta^{14}C$ values in the time interval of ~1910–1935, during which the two records exhibit well-marked, coeval decreases in $\Delta^{14}C$ in 1928 and 1932 (Fig. 2A).

Between ~1950 and 1969, coral $\delta^{13}C$ values increase and then decrease as the atmospheric values by −0.025‰/year (Fig. 2C) (*35*). The rise of $\Delta^{14}C$ in response to the atmospheric bomb ^{14}C input differs from that of published intra– and extra–Caribbean Sea coral and scleroponge records (*19*–*30*), and it appears to have two steps (Fig. 3A and figs. S1A and S2). It occurs first in 1956 in the Martinique record and about 2 to 3 years later than the atmospheric bomb $\Delta^{14}C$ rise in 1955 (*31*) in all the other records. This first rise ends by a plateau in 1959–1960 in the Martinique coral record and in 1960–1961 in the other records (figs. S2 and S3). The $\Delta^{14}C$ augments then rapidly and similarly in the western coral records [Belize (*22*), Florida (*22*–*24*, *38*), and Bahamas (*25*)] as in the Martinique record but ~2 to 3 years later in the eastern Caribbean Sea records [Puerto Rico (*26*) and Cariaco (*19*–*21*)]. The bomb-induced rise of $\Delta^{14}C$ ends in 1969 in all the coral and scleroponge records (fig. S3). Furthermore, the north-shore Bermuda (*27*–*29*) and Abrolhos (*28*) corals, each surrounded by the NAW and SAW, respectively, have much lower $\Delta^{14}C$ values than those of the Martinique coral that is bathed by a mixture of these water masses (*7*, *8*). All these features are independent of coral ages uncertainties, notably in the time interval of 1959–1969 (figs. S2 to S4). As a whole, the variations of $\delta^{13}C$ and $\Delta^{14}C$ in the Martinique coral records reveal that ocean processes dominate air-sea CO_2 exchange in the central tropical North Atlantic, as observed in the northwestern Atlantic subtropics (*29*). They may result either from local oceanic processes or from a reorganization of the tropical Atlantic circulation.

Changes of sea surface $\Delta^{14}C$ in the tropical Atlantic

In the tropical North Atlantic, the positive freshwater budget contributes to increasing salt flux, and the sea surface density gain leads to subduction into the thermocline (*39*). Thus, changes in vertical mixing between the sea surface and the low $\Delta^{14}C$ subsurface waters may explain the variations of $\Delta^{14}C$ in the Martinique coral, as well as the coeval events of $\Delta^{14}C$ lows and $\delta^{18}O_{sw}$/SSS highs.

As a test, we have adapted the multibox, isopycnal mixing model for C presented by Druffel (*29*). It contains a sea surface box that exchanges with an atmospheric box, and with three subsurface boxes to represent vertical mixing to simulate water mass renewal rate, W (year^{-1}) (fig. S7). The steady-state value of $\Delta^{14}C$ in the surface waters near Martinique Island has been calculated using the pre-1835 mean $\Delta^{14}C$ for the atmosphere (*36*), NEC (*30*), SEC (*40*), and prebomb values of the tropical subsurface waters (*41*). Using a constant mean annual value of the mixed layer depth of 40 m (*42*), the constant mean annual wind speed of 7.2 m/s (*43*), the water mass renewal (or ventilation) rate W is 0.51 year^{-1} (~20 m/year or ~1.7 year) to satisfy the steady-state value of Martinique surface $\Delta^{14}C$. Setting W to 0 and the horizontal advection to 100%, the Martinique $\Delta^{14}C$ would be more positive by 15‰ than that measured (−48.7‰) suggesting that vertical mixing acts on sea surface $\Delta^{14}C$ at Martinique Island, consistent with observations in the tropical North Atlantic (*39*).

The $\Delta^{14}C$ values of the forward model that was derived using constant values of W and horizontal advection do not differ significantly from those of the global model marine mixed layer in the pre-1950 time interval (*36*), and neither model predicts the $\Delta^{14}C$ lows (Fig. 2D). Model results also show that the Martinique $\Delta^{14}C$ values are lower than expected between 1959 and 1962 and between 1963 and 1969 (fig. S8A). The inverse model, where we calculate the W

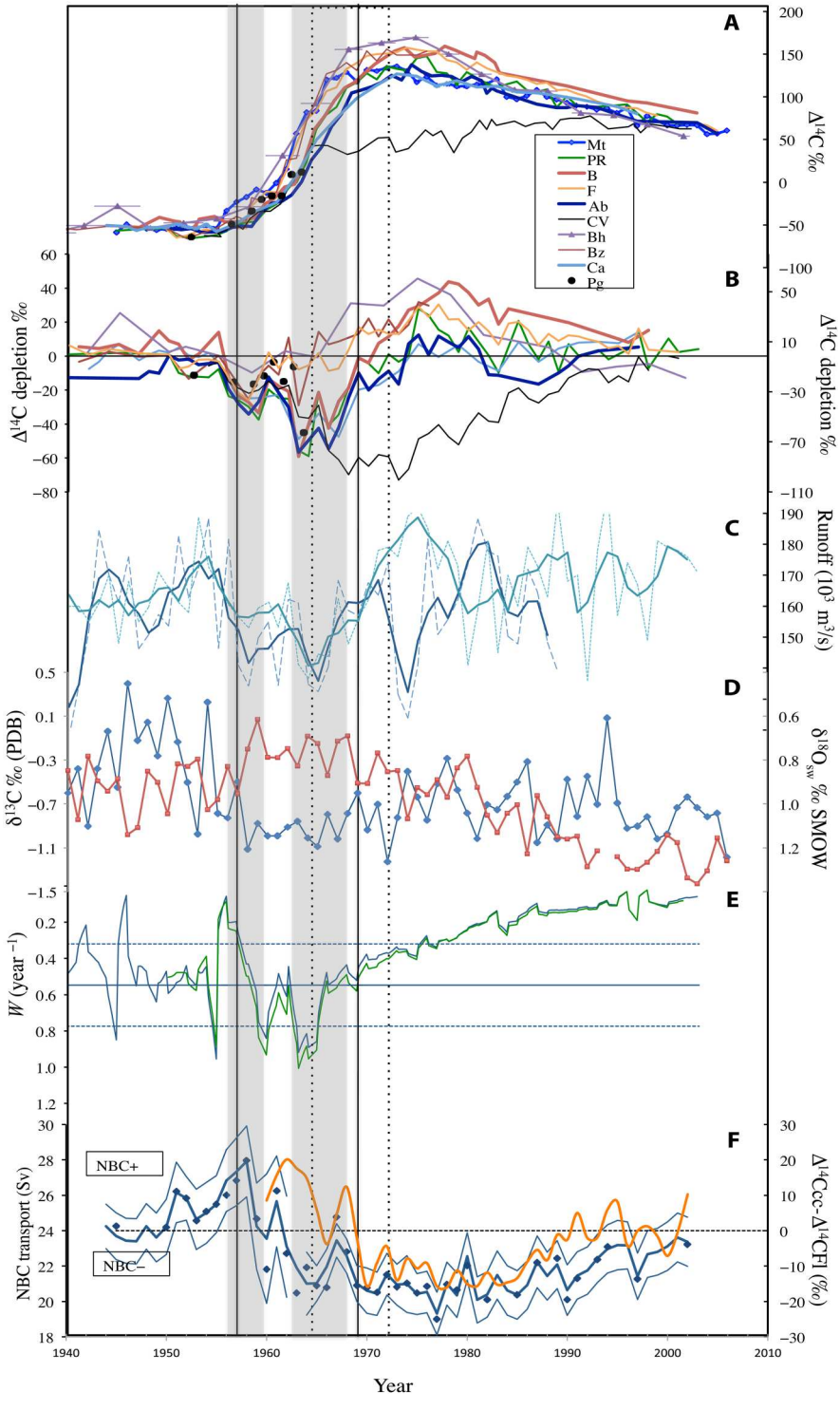

Fig. 3. Post-1940 variations of the surface water properties from oxygen and carbon isotopes and of rivers runoffs. (**A**) $\Delta^{14}C$ (‰) in coral and scleroponge bands (same legend as Fig. 1). Age uncertainties are reported for the Bahamas scleroponge (*25*). (**B**) $\Delta^{14}C$ depletion (‰) in the coral and scleroponge records relative to Martinique $\Delta^{14}C$. (**C**) Annual (dotted) and 3-year running mean (bold) discharge (10^3 m^3/s) of the Amazon (cyan) (*56*) and Orinoco (blue) (*57*) rivers with Orinoco runoff multiplied by a factor of 5 for graphic fit. (**D**) $\delta^{13}C$ (left red) and $\delta^{18}O$ (right blue) (‰ versus PDB) in the Martinique coral bands. (**E**) Vertical mixing W ($year^{-1}$; left axis, inverted scale) using the NEC $\Delta^{14}C$ changes either from the north shore Bermuda coral (blue) (*27*–*29*) or the sea surface $\Delta^{14}C$ in the southern subtropical North Atlantic (green) (box B in Fig. 1 and table S2). Thin bold and dashed blue lines represent the calculated mean values and variance of W at 2 SD between 1825 and 1835. (**F**) Annual difference (bold blue) with uncertainties at ±1σ (light blue) between the calculated $\Delta^{14}C$ of the CC water ($\Delta^{14}Ccc$) and the Florida coral bands (right axis) and model-based variations of the NBC transport (yellow) at 6°S (in Sverdrups) (left axis) (*62*). Time interval of enhanced vertical mixing W1 (black box) and of intense formation of 18° mode water (*49*) (dotted box) are shown for the entire figure. The gray boxes indicate the two steps of major $\Delta^{14}C$ decreases from 1956 to 1959 and from 1962 to 1969.

values using the observed $\Delta^{14}C$ for each year, shows a change of W in ~1968 from a mean value of 0.55 $year^{-1}$ (±0.2 $year^{-1}$ at 2 SD) to low values of 0.1 $year^{-1}$ by 1995 with small increases at the same time of the rapid step decreases in $\Delta^{14}C$. Significant pulses of increased vertical mixing occur between 1885–1895, 1925–1935, and 1958–1969, referred to as W3, W2, and W1, respectively, in Fig. 2E.

Pulse W1 (1958–1969) has occurred during a time of lower-than-normal wind speed (fig. S9) (*43*) and is likely not related to wind-induced, vertical mixing. Instead, W1 is associated with increasing $\delta^{18}O_{sw}$/SSS and sea surface density in the western tropical North Atlantic. Pulse W1 is a robust feature despite the model changes made in either the horizontal transport of surface waters or the proportions of SAW and NAW from the NBC versus NEC

or the NEC $\Delta^{14}C$ values and despite changes in the Martinique coral ages (fig. S10A). Otherwise, the $\Delta^{14}C$ in the subsurface box model are well resolved, with the exception of too high values of $\Delta^{14}C$ in the intermediate box in 1972–1973 (fig. S8B). From model results, pulse W1 may derive either from local oceanic changes or from an extended oceanic reorganization, including a change in either the advection or the $\Delta^{14}C$ value of subsurface waters or both, which is not considered by the box model calculation.

The Martinique coral and published Caribbean and extra–Caribbean Sea corals (*19*–*30*) and scleroponges (*25*) are located on the main current pathways and transport of the NAW and the SAW between ~32°N and ~18°S (Fig. 1). Analyzing the gradients of $\Delta^{14}C$ between the published records, relative to the Martinique one, provides a way to distinguish the local and regional causes of the $\Delta^{14}C$ changes in the tropical Atlantic (Fig. 3). In the North Atlantic, the four Bermuda corals from the northern (*27*–*29*) and southern shores (*30*) are bathed by the NAW from the GS. The return flows of the GS along the NEC and AC entrain the NAW to the Martinique coral and Bahamas scleroponge (*25*) sites, respectively. The NAW partly surrounds the Puerto Rico coral (*26*) by entering the Caribbean Sea through the Mona Passage (*8*). In the South Atlantic, the Abrolhos and Punta Galinha corals (*28*) are bathed by the SAW from the BC and NBC, respectively, both fed by the south SEC (*44*). The northernmost Punta Galinha coral (*28*) is additionally influenced by the westward, upwelled equatorial waters from the central SEC and north SEC. The Cape Verde coral (*25*, *28*) is in the upwelling zone of West Africa, where the SAW is from the eastward retroflection of the NBC via the North Equatorial Countercurrent and North Equatorial Undercurrent and recirculates westward along the NEC (*45*). The NBC transport of SAW and that of the Amazon and Orinoco fresh waters extend northwestward to the eastern Caribbean Sea, surrounding the Cariaco and Puerto Rico corals, similar to the Martinique coral (*11*). The Belize (*22*) and Florida (*22*–*24*, *38*) corals are located within and downstream of the CC, fed by a mixture of NAW and SAW, respectively (*7*, *8*). The transit times of sea surface flows between corals and scleroponge sites are less than 1 year (*9*). The sea surface gradients of $\Delta^{14}C$ are thus calculated between the annual growth bands in published records compared to those of the same ages at Martinique in the post-1940 time interval (Fig. 3, A and B).

Between 1940 and 1955, there are minimal differences between Martinique $\Delta^{14}C$ and other intra– and extra–Caribbean Sea records (Fig. 3B). Two $\Delta^{14}C$ decreases occur contemporaneously between 1956 and 1969. The first $\Delta^{14}C$ decrease is identical in all the coral records (~−30 to −35‰) between 1956 and 1959. The second decrease occurs between 1962 and 1969 but is of smaller amplitude (−20 and −10‰) in the western Caribbean Sea (Belize) and Florida coral records, respectively, than in the other records at −55‰. The $\Delta^{14}C$ depletion in the western Caribbean coral (Belize) ends in 1965, earlier than it does in the Puerto Rico and Bermuda coral records (1969) and in the South Atlantic and Cariaco corals (1974). Similar events are observed in the Cape Verde record, although the second one is much longer and of greater magnitude ending in 1990. By ~1990, no significant differences of $\Delta^{14}C$ exist between the coral records. The contemporaneous two-step, $\Delta^{14}C$ depletion of same amplitude in the intra– and extra–Caribbean Sea coral records, is coeval with the independently observed two steps and increases in vertical mixing during pulse W1 (lower than expected $\Delta^{14}C$) in the Martinique coral record, which excludes that they are due to uncertainties in all the coral and scleroponge ages (Fig. 3, D and E, and fig. S11).

The low $\Delta^{14}C$ values in the published coral records (*19*–*28*, *46*), relative to our Martinique record, may reflect the delayed response of surface $\Delta^{14}C$ to the atmospheric bomb $\Delta^{14}C$ rise, due to the combined effects of wind strength and depth of the mixed layer on the dilution of the atmospheric bomb $\Delta^{14}C$ into the subsurface ocean. A contemporaneous $\Delta^{14}C$ decrease in identical amplitude in all of the coral $\Delta^{14}C$ records relative to the Martinique record is opposed to delayed responses as mixing processes occur within mixed layer depth (MLD), which differs from a few tens of meters in the Caribbean Sea (*47*) to hundreds of meters at the other coral sites (*42*), such as at Bermuda (*29*). Local wind speeds are significantly lower than normal between 1956 and ~1970 in the northern sites and not significantly higher in the southern sites (fig. S12) (*43*). The $\Delta^{14}C$ lows cannot be attributed either to wind-induced turbulent vertical mixing or to wind-induced upwelling and downwelling as commonly observed along the northern and southern coasts of the Caribbean Sea, respectively (*48*), and in the off-equatorial and equatorial Atlantic upwelling zones. The interhemispheric mixing time of atmospheric $^{14}CO_2$ is ~1 year later in the southern than in the northern atmosphere (*31*), which cannot account for the late, coeval onset of the $\Delta^{14}C$ depletions in the North (Bermuda) and South Atlantic (Abrolhos) coral records. The contemporaneous and identical amplitude of the $\Delta^{14}C$ depletion in the tropical and subtropical coral records at the time of pulse W1 likely results from a large-scale reorganization of the oceanic circulation.

Origin of the $\Delta^{14}C$ lows in the tropical Atlantic and the Sub-Antarctic Mode Water

Past $\Delta^{14}C$ decreases in the northwestern subtropical NAW have been recorded in the north-shore Bermuda coral bands and attributed to intensified formation of the 18°C mode water (*27*, *29*). The southward advection of this $\Delta^{14}C$-depleted NAW would equally lower the $\Delta^{14}C$ of the intra–Caribbean Sea records, such as the Puerto Rico (*26*) record. This, however, conflicts with the high $\Delta^{14}C$ in the Martinique record, also bathed by the NAW. From hydrographic surveys starting in 1954 (*49*) and Bermuda $\Delta^{14}C$ records (*27*–*29*), one major quasi-decadal event of 18°C mode water formation occurs from 1964 to 1972, mostly later than the measured $\Delta^{14}C$ lows in the Bermuda and Puerto Rico records (Fig. 3). Moreover DIC $\Delta^{14}C$ measurements of central and southern North Atlantic subtropical waters are higher than those of the Bermuda (*27*–*29*) and Puerto Rico (*26*) records between 1966 and 1969 (boxes A and B in Fig. 1, fig. S12, and table S2). Northeastern Atlantic water $\Delta^{14}C$ are also higher than those of Bermuda and Puerto Rico records (box C in Fig. 1, fig. S12, and table S2), and they are closer to the high $\Delta^{14}C$ in the Martinique record. Intense formation of 18°C mode water and subsequent southward flow of $\Delta^{14}C$-depleted NAW cannot account very likely for the two-step, $\Delta^{14}C$ lows in the intra–Caribbean Sea records and would only account for the late $\Delta^{14}C$ depletion in the north-shore Bermuda record. The $\Delta^{14}C$ content of the SAW is strongly influenced by upwelling of subsurface waters of low $\Delta^{14}C$ and mixing with the surface waters in the eastern Atlantic margins (*41*). Only a major lowering of the SAW $\Delta^{14}C$ would explain the extent of the $\Delta^{14}C$ lows in the tropical Atlantic records from 18°S to 32°N, all interconnected by the

various branches of the SEC and the several zonal currents and undercurrents and then by the BC, NBC, CC, and GS (Fig. 1).

Pulse W1 and the $\Delta^{14}C$ lows in the tropical coral records (1956–1969) coincide with an episode of anticorrelated (cooler) subsurface and SSTs in the latitudinal band of 8° to 20°N of the tropical North Atlantic between 1950 and 1970, a unique feature in the time interval of 1950–2000 (*50*). From a global distribution of surface $\Delta^{14}C$ over time, Toggweiler *et al.* (*5*, *38*) have reported that extensive spreading of low $\Delta^{14}C$ surface water across the low-latitude Atlantic and Pacific basins should result from upwelling of the cool, low $\Delta^{14}C$ (−80‰) subsurface Sub-Antarctic Mode Water (SAMW) in eastern ocean margins, rather than from increased local upwelling. SAMW is formed in each ocean basins at 40° to 50°S by subduction of upwelled circumpolar deep water in the Southern Ocean and exported equatorward at the thermocline depth of the subtropical gyres (*51*). Intensified upwelling and northward advection of SAMW would well explain the extent of the contemporaneous, identical $\Delta^{14}C$ lows in the tropical Atlantic between 1956 and 1969 at the time of anticorrelated (cooler) subsurface and SSTs in the tropical North Atlantic (*50*). Furthermore, an unexpected abrupt increase in $\Delta^{14}C$ has been identified in 1976 during the upwelling season from a Galapagos coral record in the eastern equatorial Pacific (*52*), and ocean model experiments attributed to a decreased advection of SAMW into the equatorial undercurrent where they upwell (*53*). This almost coincides with the end of the $\Delta^{14}C$ depletion in the South Atlantic (Abrolhos) (*28*) and southern Caribbean [Cariaco (*19*–*21*)] records and with the onset of its resumption in the Cape Verde record in ~1974 (Fig. 3B). The resumption of the Cape Verde $\Delta^{14}C$ depletion, relative to the subtropical (Bermuda) one, has been previously dated in 1980 and attributed to a ~20-year delay of bomb $\Delta^{14}C$ penetration into the eastern Atlantic thermocline (*25*). This cannot account for both the contemporaneous, identical sea surface $\Delta^{14}C$ lows in the tropical Atlantic coral records, relative to the Martinique $\Delta^{14}C$, and current drifts. The upper thermocline in the eastern Atlantic is supplied by water of South Atlantic origin (*45*). The $\Delta^{14}C$ lows originate very likely from an anomalous episode of enhanced northward advection and upwelling of the cool, $\Delta^{14}C$-depleted subsurface SAMW to the tropical North Atlantic from 1956 to 1969. They are likely of global significance, and they are associated with a change in the tropical Atlantic current transport.

The widespread northward advection of SAMW has deeply changed the hydrographic and isotopic properties of the tropical Atlantic waters and climate of the surroundings at the time of the $\Delta^{14}C$ lows and pulse W1 (1956–1969) (Fig. 3). Cooler South Atlantic (0 to 20°S) than North Atlantic SSTs (0 to 25°N) have been observed between ~1950 and 1965 (*54*). This dipole distribution of SSTs affects the rainfall patterns over the Amazonian basin with cold (warm) South Atlantic SSTs associated with decreased (increased) precipitation (*55*), reducing (increasing) the river runoff. A decrease in the two river runoffs between 1955 and 1970 (*56*, *57*) matches the two-step, $\Delta^{14}C$ depletion in the Cariaco and Puerto Rico coral bands, both influenced by the Amazon and Orinoco freshwater plumes (*10*), similarly as the Martinique coral (Fig. 3, B and C). The high $\delta^{18}O_{sw}$/SSS (high *W*) values in the Martinique coral bands also coincide with reduced river discharges, consequently reduced northward transport of the Amazon and Orinoco fresh waters of light DIC $\delta^{18}O$ (Fig. 3, C and D) (*32*, *58*). The high $\delta^{13}C$ conflicts with a reduced transport of the nutrient-rich Amazon and Orinoco rivers (Figs. 2C and 3, C and D). This limits nutrient availability for coral algae symbionts, which preferentially use ^{12}C during photosynthesis and leave ^{13}C for coral skeleton growth (*17*). The high $\delta^{13}C$ may result from a change in seawater DIC $\delta^{13}C$ (*17*). The SAMWs are characterized by high DIC $\delta^{13}C$ due to fractionation at cold temperature (*59*). Combined with the preferential evasion of the ^{12}C due to insufficient time for equilibration at warm temperatures (*60*), the upwelling of SAMW and mixing with the sea surface in the Atlantic may have contributed to increase DIC $\delta^{13}C$ of seawater leading to the increase in $\delta^{13}C$ in coral skeleton associated with low $\Delta^{14}C$.

Past changes of the carbon and oxygen isotopic values and of *W* in the Martinique records between 1885 and 1895 and between 1925 and 1935 are also compatible with the oceanic and climatic impacts of major episodes of SAMW advection and upwelling throughout the Atlantic. They are associated with time intervals of cooler SSTs in the South Atlantic than in the North Atlantic (*54*) and between 1925 and 1935 to low river discharges of the Amazon and Orinoco fresh waters (fig. S4) (*56*, *57*).

Changes in the CC transport and MOC

The high Martinique $\Delta^{14}C$ values relatively to the low intra–Caribbean Sea ones from 1956 to 1969 emphasize a major change in the tropical Atlantic current transport. Changes in the relative transports of NAW and SAW into the Caribbean Sea can be approximated by calculating the $\Delta^{14}C$ values of the CC ($\Delta^{14}Ccc$) upstream of the Yucatan Strait and by comparing them with those of the downstream Florida coral (see Materials and Methods and fig. S13) (*22*–*24*, *38*). The annual changes of $\Delta^{14}Ccc$ are calculated from a simple mixing equation using the modern Atlantic transports through the Antilles passages into the Caribbean Sea (*8*) and the values of $\Delta^{14}C$ of the NAW and SAW inflows as recorded by the northern [Bahamas (*25*) and Puerto Rico (*26*)], eastern (Martinique) and southeastern [Cariaco (*19*–*21*) or Abrolhos (*28*)] scleroponge and corals. As coral $\Delta^{14}C$ values reflect those of the surrounding seawater DIC, the deviation of $\Delta^{14}Ccc$ from the Florida $\Delta^{14}C$ (*22*–*24*, *38*) would express the changes of the NAW and SAW inflows into the Caribbean Sea. A positive (negative) $\Delta^{14}C$ deviation indicates a too weak (strong) transport of the $\Delta^{14}C$-depleted SAW into the CC, relatively to a too strong (weak) transport of NAW (Fig. 3F).

The deviation of $\Delta^{14}Ccc$ from the Florida coral $\Delta^{14}C$ reflects adequately the observed modern transports of NAW and SAW into the CC as it is close to zero beyond ~1990. Modern-like transports also prevail between 1945 and 1950, as shown by the null deviation. A significant change occurs in 1962 from about +20‰ in 1957–1958 to −20‰ between 1963 and 1969. It is still −20‰ until 1985 and becomes negligible in the mid-90s. To match the Florida $\Delta^{14}C$, the NBC transport of the $\Delta^{14}C$-depleted SAW into the CC relatively to the inflow of NAW should increase in 1957–1958 and then decrease between 1963 and 1969. This is consistent with hydrographic (*61*) and model-based observations (*62*) of the NBC transport (Fig. 3F). The $\Delta^{14}C$ deviation of $\Delta^{14}Ccc$ from the Florida $\Delta^{14}C$ mirrors the model-based variations of the NBC transport, as estimated at 6°S in the 0- to 1200-m water depth (*62*), with a correlation coefficient r^2 of 0.40 between 1960 and 2002.

In addition, the decrease in the NBC transport of SAW into the Caribbean Sea should be counterbalanced by an increase in the NAW one between 1963 and 1969, as the values of $\Delta^{14}Ccc$ should match the Florida ones (*22*–*24*, *38*). However, the $\Delta^{14}C$ depletion of

the downstream Puerto Rico record (*26*), relative to the Martinique one, implies a weakening of the westward transport of NAW between 1963 and 1969 (Fig. 3, A and B). Likewise, the greater $\Delta^{14}C$ depletion in the eastern Caribbean [Puerto Rico (*26*) and Cariaco (*19*–*21*)] records than in the downstream western Caribbean (Belize) (*22*) and Florida (*22*–*24*, *38*) records denotes a slowdown of the CC transport to the western Caribbean Sea and Gulf of Mexico between 1963 and 1969. The $\Delta^{14}C$ depletion in the intra–Caribbean Sea records would be therefore associated with a decrease in the NEC, NBC, and CC transports between 1963 and 1969, in agreement with observations of a reduced transport of the Florida Current from the early 1960s to the mid-70s (*63*). Moreover, climate model–hindcast results of MOC transport in the Atlantic Ocean (*6*) have evidenced a strong decrease in the interhemispheric transport likely of southern origin in the early 1960s with a major slow down between ~1965 and ~1968.

The irregular decadal, double-peak changes of oxygen and carbon isotopes and of *W* in the Martinique coral records begin in 1885. These changes coincide with the onset of an anomalous weak Labrador Sea convection and Atlantic overturning circulation (OC) in 1880, compared with the preceding 1600 years (*64*). The 11-year running means of the $\Delta^{14}C$ and OC-proxy records are significantly correlated by a ~28-year lead or lag of the $\Delta^{14}C$ between 1880 and 1955 (fig. S14). Model-based transit times of the upper MOC transport from the South to the North Atlantic at 20°N show a double-peak distribution at 19 and 29 years (*65*) due to direct transports from the Drake Passage (*65*) and from South of Africa via the Agulhas Current (*66*) and to the recirculation along the South Atlantic gyre, respectively (*65*). The latter transit time is equal to the lead/lag of ~28 years between the decadal changes of the $\Delta^{14}C$ and OC-proxy records, which reinforces the inferred Southern origin of the measured $\Delta^{14}C$ lows in the Martinique coral record. The double-peak structure of the decadal $\Delta^{14}C$ lows in the Martinique coral record could reflect the 10-year spaced double-peak distribution of the upper MOC transport. From the modeled transit times, previous episodes of enhanced formation of low $\Delta^{14}C$ SAMW would have taken place in 1906 and 1937 to initiate the two last North Atlantic tropical $\Delta^{14}C$ lows (1925–1935 and 1956–1969) (table S3). This is compatible with earlier observations of enhanced wind-driven upwelling of cold and ^{14}C-depleted waters up to the sea surface in the Southern Ocean between 1900 and 1940 (*67*). Contemporaneous upwelling is observed in the different ocean basins of the Southern Ocean that has likely contributed to enhanced formation of low $\Delta^{14}C$ SAMW. Although other mechanisms may be responsible, the irregular, double peaks of the Martinique $\Delta^{14}C$ lows might be a direct consequence of sporadic recovery of a stronger OC in the North Atlantic as observed earlier in the 19th century (*63*), a stronger MOC instigating the northward inflow of low $\Delta^{14}C$ SAMW into the tropical basins. Otherwise, the formation and transport of the low-$\Delta^{14}C$ SAMW into the tropical Atlantic might be the result of wind-induced oceanic changes, such as upwelling or subsurface Pacific and Indian leakages (*4*–*6*) in the Southern Ocean and of a northward transport through various export pathways and transit times (table S3).

Overall, the carbon and oxygen isotope records in the Martinique coral bands, extending back to 1825 CE, reveal irregular, decadal oceanic changes of $\Delta^{14}C$, salinity, and vertical mixing in the tropical North Atlantic, starting in 1885. The post-1950 record of Martinique $\Delta^{14}C$ differs from other published $\Delta^{14}C$ records, highlighting widespread $\Delta^{14}C$ lows of South Atlantic origin in the tropical Atlantic waters from 18°S to 32°N between 1956 and 1969. These changes and the past Martinique ones are attributed to the northward advection of the low $\Delta^{14}C$ SAMW, formed in the Southern Ocean. Consequences are reduced Amazon and Orinoco runoff (*56*, *57*) and limited advection of the river freshwater into the tropical North Atlantic as shown by high $\delta^{18}O/\delta^{18}O_{sw}$ and saltier surface waters.

The last event of SAMW advection into the tropical North Atlantic (1956–1969) coincides with the onset of intense formation of 18°C mode water in the northwestern subtropical North Atlantic (*27*, *29*, *49*). It is concurrent with a major slowdown of the CC transport between 1963 and 1969 and of the MOC (*6*). The decadal pulses of low $\Delta^{14}C$ in the Martinique coral record starts in 1885 at the onset of a centennial-scale weakening of the Labrador Sea convection and Atlantic OC, and they are a direct consequence of decadal MOC changes since 1880. Extended records of carbon and oxygen isotopes into older ages and across various ocean basins, notably the Southern Ocean, provide a way to monitor centennial-scale, interhemispheric variations of MOC, providing a better knowledge of their linkage with climate change. Our observations of decadal oceanic changes in the tropical North Atlantic since 1825 CE reveal the importance of long-term natural changes of the oceanic circulation that may be accounted for in model forecasts of climate change.

MATERIALS AND METHODS

The Martinique coral Chancel 1, *S. siderea*, of a microatoll shape was collected alive in January 2008 at a water depth of ~1.50 m on the Atlantic coast of Martinique Island at îlet Chancel (14°70 N, 60°90 W) (*14*). The coral slab cut extends over a ~1 m in length (*68*). Chronology is based on the counting of the annual growth bands and Th/U dating (*68*) on the correlation of die down surfaces of a series of corals from microatoll sampled south of the Caravelle Peninsula (*14*). In addition, two chronological markers are provided by coeval changes of the coral $\delta^{18}O_{sw}$/salinity and of the Amazon and Orinocco runoff (fig. S4) (*56*, *57*).

Oxygen and carbon isotope measurements

These analyses have been performed on subsamples of the same annual bands of the Martinique coral growth. A chemical pretreatment of the coral powder was done for radiocarbon analyses using HNO_3 (0.01 N) and the carbonate hydrolyzed with H_3PO_4 in a semiautomatic vacuum line were performed at the Gif-LSCE Radiocarbon Laboratory (*69*). Graphite targets were prepared and measured at the French National AMS-ARTEMIS-LMC14 facility (*70*). Results are expressed in age-corrected $\Delta^{14}C$ (‰), which is the deviation in parts per thousand (‰) of a sample's $^{14}C/^{12}C$ ratio of known age from that of the absolute standard activity in 1950 (*15*). The $\Delta^{14}C$ uncertainty is 3 to 4‰. The oxygen and carbon isotopes were analyzed on coral powders at the LSCE, using an Optima-VG mass spectrometer (isotope ratio mass spectrometer) coupled with a common acid bath and an automated preparation line to produce CO_2. The isotope compositions were calibrated against the NBS 18 and 19 standards. Oxygen and carbon isotopic compositions are reported in the classical notation and expressed in per mil (‰) versus PDB (Pee Dee Belemnite). The

external precision is 0.02 and 0.04‰ (1σ) for carbon and oxygen, respectively.

The oxygen isotope values of seawater ($\delta^{18}O_{sw}$ per mil versus standard mean ocean values) have been calculated using the SSTs from ERSST.V3b (*71*, *72*) measured at nearly the same water depth as that of the coral and a temperature fractionation of 0.19‰/°C from Watanabe's equation (figs. S5 and S6) (*16*). The changes in SSS have been estimated using Watanabe's $\delta^{18}O_{sw}$/salinity relationship (*16*).

Calculation of the Δ^{14}Ccc

The annual Δ^{14}C record for the CC (Δ^{14}Ccc) has been calculated by a simple mixing equation using the inflow distribution in the northern, eastern, and southeastern Caribbean Sea passages, which supplies the CC (*8*) and the Δ^{14}C values of these inflows, as recorded by the corals and scleroponge, located close to the main passages (fig. S13). According to Johns *et al.* (*8*), the inflow feeding the CC through the northern Lesser Antilles is 8.3 Sv (30% of the total inflow at 28.3 Sv), and the Δ^{14}C has been set on the Martinique Δ^{14}C. The southern inflow is summed at 10.1 Sv (35%), and the Δ^{14}C has been set on the Cariaco (*19*–*21*) and Abrolhos (*28*) coral Δ^{14}C. The northern Atlantic inflow through the Windward Passage is 7 Sv (25%) and linked to the Bahamas (*25*) Δ^{14}C and 3 Sv (10%) through the Mona Passage and related to the Puerto Rico coral (*26*) Δ^{14}C. The sea surface flow at the Yucatan Strait is about 30% of the total transport down to the sill depth (*8*) similar to that in the southern Lesser Antilles passages at about 33% (*18*). Thus, we estimate that this ratio is the same for each Atlantic inflow into the CC through the Antilles passages (*8*), and the values of Δ^{14}Ccc have been calculated using the relative proportions of the total transports in the Atlantic passages.

As the annual values of Florida Δ^{14}C record (*22*–*24*, *38*) do not differ significantly from those of corals located in the northern and western Gulf of Mexico (*21*) at the time of the two-step, Δ^{14}C depletion, the deviation of Δ^{14}Ccc from the Florida Δ^{14}C mainly reflects the upstream changes of NAW versus SAW in the CC. The calculation has been done at constant transports, except between 1955 and 1969. The inflow through the Mona Passage has been set to 0 Sv because the Puerto Rico coral Δ^{14}C record is more Δ^{14}C-depleted than that of the eastern NAW inflow as shown by the Martinique coral (see the section "Origin of the Δ^{14}C lows"). This does not significantly change the Δ^{14}C difference between Δ^{14}Ccc and Florida Δ^{14}C because the inflow of NAW near the Puerto Rico coral location is only 10% of the total inflow. The correlation coefficient r^2 between the model-based NBC transport (*62*) and the Δ^{14}C deviation between Δ^{14}Ccc and Florida Δ^{14}C are 0.40. The uncertainties on Δ^{14}Ccc have been calculated at ±1σ considering that the corals and scleroponge have independent Δ^{14}C values, while the errors on the Δ^{14}C deviations between Δ^{14}Ccc and Florida Δ^{14}C are the square root of the squared analytical errors.

Shifting the coral ages toward younger ages does not strongly change the offset between Δ^{14}Ccc and Florida Δ^{14}C (fig. S10B). It is slightly positive at ~10‰ between 1950 and 1962, while initially at 20‰, and significantly negative between 1963 and 1969, as observed with the initial chronology. The fluctuations of this offset mirror those of the NBC transport (*62*), and the correlation is still unchanged and significant (r^2 = 0.40).

Supplementary Materials

This PDF file includes:

Supplementary Text
Figs. S1 to S14
Table S3
Legends for tables S1 and S2
References

Other Supplementary Material for this manuscript includes the following:

Tables S1 and S2

REFERENCES AND NOTES

1. M. S. Lozier, Overturning in the North Atlantic. *Ann. Rev. Mar. Sci.* **4**, 291–315 (2012).
2. M. W. Buckley, J. Marshall, Observations, inferences, and mechanisms of the Atlantic meridional overturning circulation: A review. *Rev. Geophys.* **54**, 5–63 (2016).
3. M. S. Lozier, V. Roussenov, M. S. C. Reed, R. G. Williams, Opposing decadal changes for the North Atlantic meridional overturning circulation. *Nat. Geosci.* **3**, 728–734 (2010).
4. A. Biastoch, C. W. Böning, J. R. E. Lutjeharms, Agulhas leakage dynamics affects decadal variability in Atlantic overturning circulation. *Nature* **456**, 489–492 (2008).
5. J. R. Toggweiler, E. R. M. Druffel, R. M. Key, E. D. Galbraith, Upwelling in the ocean basins north of the ACC: 2. How cool subantarctic water reaches the surface in the tropics. *J. Geophys. Res. Oceans.* **124**, 2609–2625 (2019a).
6. A. Biastoch, F. U. Schwarzkopf, K. Getzlaff, S. Rühs, T. Martin, M. Scheinert, T. Schulzki, P. Handmann, R. Hummels, C. W. Böning, Regional imprints of changes in the Atlantic meridional overturning circulation in the eddy-rich ocean model VIKING20X. *Ocean Sci.* **17**, 1177–1211 (2021).
7. W. J. Schmitz, P. L. Richardson, On the sources of the Florida current. *Deep Sea Res. A. Oceanogr. Res. Pap.* **38**, S379–S409 (1991).
8. W. E. Johns, T. L. Townsend, D. M. Fratantoni, W. D. Wilson, On the Atlantic inflow to the Caribbean Sea. *Deep Sea Res. I Oceanogr. Res. Pap.* **49**, 211–243 (2002).
9. D. M. Fratantoni, North Atlantic surface circulation during the 1990's observed with satellite-tracked drifters. *J. Geophys. Res.* **106**, 22067–22093 (2001).
10. F. L. Hellweger, A. L. Gordon, Tracing Amazon River water into the Caribbean Sea. *J. Mar. Res.* **60**, 537–549 (2002).
11. A. Dessier, J. R. Donguy, The sea surface salinity in the tropical Atlantic between 10°S and 30°N— Seasonal and interannual variations (1977–1989). *Deep-Sea Res, Part I.* **41**, 81–100 (1994).
12. M. Vellinga, P. Wu, Low-latitude freshwater influence on centennial variability of the Atlantic thermohaline circulation. *J. Climate* **17**, 4498–4511 (2004).
13. S. Jahfer, P. N. Vinayachandran, R. S. Nanjundiah, Long-term impact of Amazon river runoff on northern hemispheric climate. *Nat. Commun.* **7**, 10989 (2017).
14. J. Weil-Accardo, N. Feuillet, E. Jacques, P. Deschamps, F. Beauducel, G. Cabioch, P. Tapponnier, J. M. Saurel, J. Galetzka, Two hundred thirty years of relative sea level changes due to climate and megathrust tectonics recorded in coral microatolls of Martinique (French West Indies). *J. Geophys. Res. Solid Earth* **121**, 2873–2903 (2016).
15. M. Stuiver, H. A. Polach, Discussion reporting of ^{14}C data. *Radiocarbon* **19**, 355–363 (1977).
16. T. Watanabe, A. Winter, T. Oba, Seasonal changes in sea surface temperature and salinity during the Little Ice Age in the Caribbean Sea deduced from Mg/Ca and $^{18}O/^{16}O$ ratios in corals. *Mar. Geol.* **173**, 21–35 (2001).
17. P. K. Swart, L. Greer, B. E. Rosenheim, C. S. Moses, A. J. Waite, A. Winter, R. E. Dodge, K. Helmle, The ^{13}C Suess effect in scleractinian corals mirror changes in the anthropogenic CO_2 inventory of the surface oceans. *Geophys. Res. Lett.* **37**, L05604 (2010).
18. M. Rhein, K. Kirchner, C. Mertens, R. Steinfeldt, M. Walter, M. U. Fleischmann-Wischnath, Transport of South Atlantic water through the passages South of Guadeloupe and across 16°N, 2000–2004. *Deep Sea Res. I Oceanogr. Res. Pap.* **52**, 2234–2249 (2005).
19. T. P. Guilderson, J. E. Cole, J. R. Southon, Pre-bomb Δ^{14}C variability and the Suess effect in Cariaco Basin surface waters as recorded in hermatypic corals. *Radiocarbon* **47**, 57–65 (2005).
20. A. J. Wagner, T. P. Guilderson, N. C. Slowey, J. E. Cole, Prebomb surface water radiocarbon of the Gulf of Mexico and Caribbean as recorded in hermatypic corals. *Radiocarbon* **51**, 947–954 (2009).
21. A.J. Wagner, "Oxygen and carbon isotopes and coral growth in the Gulf of Mexico and Caribbean Sea as environmental and climate indicators," dissertation, Department of Oceanography, Texas A&M University (2009).
22. E. R. M. Druffel, Radiocarbon in annual coral rings of Belize and Florida. *Radiocarbon* **22**, 363–371 (1980).

23. E. R. M. Druffel, T. W. Linick, Radiocarbon in annual coral rings of Florida. *Geophys. Res. Lett.* **5**, 913–916 (1978).
24. E. R. M. Druffel, H. E. Suess, On the radiocarbon record in banded corals: Exchange parameters and net transport of $^{14}CO_2$ between atmosphere and surface ocean. *J. Geophys. Res.* **88**, 1271–1280 (1983).
25. A. Fernandez, T. J. Lapen, R. Andreasen, R. P. K. Swart, C. D. White, B. E. Rosenheim, Ventilation time scales of the North Atlantic subtropical cell revealed by coral radiocarbon from the Cape Verde Islands. *Paleoceanography* **30**, 938–948 (2015).
26. K. H. Kilbourne, T. M. Quinn, T. P. Guilderson, R. S. Webb, F. W. Taylor, Decadal- to interannual-scale source water variations in the Caribbean Sea recorded by Puerto Rican coral radiocarbon. *Climate Dynam.* **29**, 51–62 (2007).
27. E. R. M. Druffel, Decade time scale variability of ventilation in the North Atlantic: High-precision measurements of bomb radiocarbon in banded corals. *J. Geophys. Res.* **94**, 3271–3285 (1989).
28. E. R. M. Druffel, Post-bomb radiocarbon records of surface corals from the tropical Atlantic Ocean. *Radiocarbon* **38**, 563–572 (1996).
29. E. R. M. Druffel, Pulses of rapid ventilation in the North Atlantic surface ocean during the past century. *Science* **275**, 1454–1457 (1997).
30. N. Goodkin, E. R. M. Druffel, K. A. Hughen, S. C. Doney, Two centuries of limited variability in subtropical North Atlantic thermocline ventilation. *Nat. Commun.* **3**, 803 (2012).
31. Q. Hua, M. Barbetti, A. Z. Rakowski, Atmospheric radiocarbon for the period 1950—2010. *Radiocarbon* **55**, 2059–2072 (2013).
32. G. A. Schmidt, G. R. Bigg, E. J. Rohling, "Global seawater oxygen-18 database - v1.21" (1999); https://data.giss.nasa.gov/o18data/.
33. G. Reverdin, E. Kestenare, C. Frankignoul, T. Delcroix, Surface salinity in the Atlantic Ocean (30°S–50°N). *Prog. Oceanogr.* **73**, 311–340 (2007).
34. E. R. M. Druffel, L. M. Benavides, Input of excess CO_2 to the surface ocean based on $^{13}C/^{12}C$ ratios in a banded Jamaican sclerosponge. *Nature* **321**, 58–61 (1986).
35. M. Rubino, M. Etheridge, C. M. Trudinger, C. E. Allison, M. O. Battle, R. L. Langenfelds, L. P. Steele, M. Curran, M. Bender, J. W. C. White, T. M. Jenk, T. Blunier, R. J. Francey, A revised 1000 year atmospheric $\delta^{13}C$-CO_2 record from Law Dome and South Pole, Antarctica. *J. Geophys. Res-Atmos.* **118**, 8482–8499 (2013).
36. M. Stuiver, P. J. Reimer, T. F. Braziunas, High-precision radiocarbon age calibration for terrestrial and marine samples. *Radiocarbon* **40**, 1127–1151 (1998).
37. W. S. Broecker, T. H. Peng, Gas exchange rates between air and sea. *Tellus* **26**, 21–35 (1974).
38. J. R. Toggweiler, E. R. M. Druffel, R. M. Key, E. D. Galbraith, Upwelling in the ocean basins north of the ACC: 1. On the upwelling exposed by the surface distribution of $\Delta^{14}C$. *J. Geophys. Res. Oceans.* **124**, 2591–2608 (2019).
39. R. W. Schmitt, P. S. Bogden, C. E. Dorman, Evaporation minus precipitation and density fluxes for the North Atlantic. *J. Phys. Oceanogr.* **19**, 1208–1221 (1989).
40. C. A. Lewis, P. J. Reimer, R. W. Reimer, Marine reservoir corrections: St. Helena, South Atlantic Ocean. *Radiocarbon* **50**, 275–280 (2008).
41. W. S. Broecker, R. Gerard, M. Ewing, B. C. Heezen, Natural radiocarbon in the Atlantic Ocean. *J. Geophys. Res.* **65**, 2903–2931 (1960).
42. C. Boyer Montégut, G. Madec, A. S. Fischer, A. Lazar, D. Iudicone, Mixed layer depth over the global ocean: An examination of profile data and a profile-based climatology. *J. Geophys. Res.* **109**, C12003 (2004).
43. E. Kalnay, M. Kanamitsu, R. Kistler, W. Collins, D. Deaven, L. Gandin, M. Iredell, S. Saha, G. White, J. Woollen, Y. Zhu, M. Chelliah, W. Ebisuzaki, W. Higgins, J. Janowiak, K. C. Mo, C. Ropelewski, J. Wang, A. Leetmaa, R. Reynolds, R. Jenne, D. Joseph, The NCEP/NCAR 40-year reanalysis project. *Bull. Amer. Meteor. Soc.* **77**, 437–471 (1996).
44. L. Stramma, F. Schott, The mean flow of the tropical Atlantic Ocean. *Deep-Sea Res, Part II.* **46**, 279–303 (1999).
45. J. E. Pena-Izquierdo, J. L. van Sebille, J. Pelegrı, E. Sprintall, P. J. Mason, P. J. Llanillo, F. Machin, Water mass pathways to the North Atlantic oxygen minimum zone. *J. Geophys. Res. Oceans* **120**, 3350–3372 (2015).
46. R. Schlitzer, "Ocean data view" (2018); https://odv.awi.de.
47. R. A. Montoya-Sanchez, A. Devis-Morales, G. Bernall, G. Poveda, Seasonal and interannual variability of the mixed layer heat budget in the Caribbean Sea. *J. Mar. Syst.* **187**, 111–127 (2018).
48. A. L. Gordon, Circulation of the Caribbean Sea. *J. Geophys. Res.* **72**, 6207–6223 (1967).
49. L. D. Talley, M. E. Raymer, Eighteen degree water variability. *J. Mar. Res.* **40**, 757–775 (1982).
50. C. Wang, L. Zhang, Multidecadal ocean temperature and salinity variability in the tropical North Atlantic: Linking with the AMO, AMOC, and subtropical cell. *J. Climate* **26**, 6137–6162 (2013).
51. K. Hanawa, L. D. Talley, Mode waters, in *Ocean Circulation and Climate*, G. Siedler, J. Church, J. Gould, Eds. (Academic Press, 2001), pp. 373–386.
52. T. P. Guilderson, D. Schrag, Abrupt shift in subsurface temperatures in the tropical Pacific associated with changes in El Niño. *Science* **281**, 240–243 (1998).
53. K. Rodgers, B. Blanke, G. Madec, O. Aumont, P. Ciais, J.-C. Dutay, Extratropical sources of equatorial Pacific upwelling in an OGCM. *Geophys. Res. Lett.* **30**, 1084 (2003).
54. D. B. Enfield, A. M. Mestas-Nunez, D. A. Mayer, L. Cid-Serrano, How ubiquitous is the dipole relationship in tropical Atlantic sea surface temperatures? *J. Geophys. Res.* **104**, 7841–7848 (1999).
55. S.-P. Xie, J. A. Carton, Tropical Atlantic variability: Patterns, mechanisms, and impacts, in *Earth Climate: The Ocean-Atmosphere Interaction*, C. Wang, S.-P. Xie, J. A. Carton, Eds. (Geophysical Monograph Series, AGU, 2004), pp. 121–142.
56. C. J. Vorosmarty, B. M. Fekete, B. A. Tucker, "Global River Discharge, 1807-1991, V. 1.1 (RivDIS). ORNL DAAC, Oak Ridge, Tennessee, USA" (1998); https://doi.org/10.3334/ORNLDAAC/199.
57. J. Callede, J. L. Guyot, J. Ronchail, M. Molinier, E. De Oliveira, L'Amazone à Óbidos (Brésil): Étude statistique des débits et bilan hydrologique. *Hydrol. Sci. J.* **47**, 321–333 (2002).
58. E. R. M. Druffel, J. E. Bauer, S. Griffin, Input of particulate organic and dissolved inorganic carbon from the Amazon to the Atlantic Ocean. *Geochem. Geophys. Geosyst.* **6**, Q03009 (2005).
59. M. Eide, A. Olsen, U. S. Ninnemann, T. Johannessen, A global ocean climatology of preindustrial and modern ocean $\delta^{13}C$. *Global Biogeochem. Cycles* **31**, 515–534 (2017).
60. J. Lynch-Stieglitz, T. F. Stocker, W. S. Broecker, R. G. Fairbanks, The influence of air-sea exchange on the isotopic composition of oceanic carbon: Observations and modeling. *Global Biogeochem. Cycles* **9**, 653–665 (1995).
61. D. Zhang, R. Msadek, M. J. McPhaden, T. Delworth, Multidecadal variability of the North Brazil Current and its connection to the Atlantic meridional overturning circulation. *J. Geophys. Res.* **116**, C04012 (2011).
62. S. Rühs, K. Getzlaff, J. V. Durgadoo, A. Biastoch, C. W. Böning, On the suitability of North Brazil Current transport estimates for monitoring basin-scale AMOC changes. *Geophys. Res. Lett.* **42**, 8072–8080 (2015).
63. C. S. Meinen, M. O. Baringer, R. F. Garcia, Florida current transport variability: An analysis of annual and longer-period signals. *Deep Sea Res. Part I* **57**, 835–846 (2010).
64. D. J. R. Thornalley, D. W. Oppo, P. Ortega, J. I. Robson, C. M. Brierley, R. Davis, I. R. Hall, P. Moffa-Sanchez, N. L. Rose, P. T. Spooner, I. M. Yashayaev, L. D. Keigwin, Anomalously weak Labrador Sea convection and Atlantic overturning during the past 150 years. *Nature* **556**, 227–230 (2018).
65. S. Speich, B. Blanke, G. Madec, Warm and cold water routes of an O.G.C.M. Thermohaline Conveyor Belt. *Geophys. Res. Lett.* **28**, 311–314 (2001).
66. S. Rühs, F. U. Schwarzkopf, S. Speich, A. Biastoch, Cold vs. warm water route – Sources for the upper limb of the Atlantic meridional overturning circulation revisited in a high-resolution ocean model. *Ocean Sci.* **15**, 489–512 (2019).
67. M. Paterne, E. Michel, V. Héros, Variability of marine ^{14}C reservoir ages in the Southern Ocean highlighting circulation changes between 1910 and 1950. *Earth Planet. Sci. Lett.* **511**, 99–104 (2019).
68. M. Paterne, N. Feuillet, G. Cabioch, E. Cortijo, D. Blamart, J. Weill-Accardo, L. Bonneau, C. Colin, E. Douville, E. Pons-Branchu, Reservoir ages in the western tropical North Atlantic from one coral off Martinique Island (Lesser Antilles). *Radiocarbon* **60**, 639–652 (2018).
69. N. Tisnérat-Laborde, J. J. Poupeau, J. F. Tannau, M. Paterne, Development of a semi-automated system for routine preparation of carbonate samples. *Radiocarbon* **43**, 299–304 (2001).
70. C. Moreau, I. Caffy, C. Comby, E. Delqué-Kolic, J. P. Dumoulin, S. Hain, J. Vincent, Research and development of the Artemis ^{14}C AMS facility: Status report. *Radiocarbon* **55**, 331–337 (2013).
71. T. M. Smith, R. W. Reynolds, T. C. Peterson, J. Lawrimore, Improvements to NOAA's historical merged land-ocean surface temperature analysis (1880-2006). *J. Climate* **21**, 2283–2296 (2008).
72. Y. Xue, T. M. Smith, R. W. Reynolds, Interdecadal changes of 30-yr SST normals during 1871-2000. *J. Climate* **16**, 1601–1612 (2003).
73. W. S. Broecker, E. A. Olson, Radiocarbon from nuclear tests, II. *Science* **132**, 712–721 (1960).
74. H. G. Ostlund, L. G. Engstrand, Stockholm natural radiocarbon measurements V. *Radiocarbon* **5**, 203–227 (1963).
75. W. S. Broecker, E. A. Olson, Lamont radiocarbon measurements VIII. *Radiocarbon* **3**, 176–204 (1961).
76. The Carina Group, "CARINA Data Synthesis Project"; www.ncei.noaa.gov/access/ocean-carbon-acidification-data-system/oceans/CARINA/about_carina.html
77. T. D. Mathews, A. D. Fredericks, W. M. Sackett, The geochemistry of radiocarbon in the Gulf of Mexico. AIEA-SM-158/48, 725–734 (1973).
78. W. Ribbat, K. O. Roether, Turnover of eastern Caribbean deep water from ^{14}C measurements. *Earth Planet. Sci. Lett.* **32**, 331–341 (1976).

79. W. Fairhall, A. W. Young, Young historical ^{14}C measurements from the Atlantic, Pacific, and Indian oceans. *Radiocarbon* **27**, 473–507 (1985).
80. R. Nydal, Carbon-14 measurements in surface water CO_2 from the Atlantic, Indian and Pacific Oceans, 1965–1994. R. Nydal, A. L. Brenkert (ed.), and T. A. Boden (ed. ORNL/CDIAC-104, NDP-057A. Carbon Dioxide Information Analysis Center, Oak Ridge National Laboratory Oak Ridge, Tennessee, USA pp. 131. doi: 10.3334/CDIAC/otg.ndp057 (1998).
81. C. L. Sabine, R. M. Key, A. Kozyr, R. A. Feely, R. Wanninkhof, F. J. Millero, T.-H. Peng, J. L. Bullister, K. Lee, "Global Ocean Data Analysis Project (GLODAP): Results and data," Carbon Dioxide Information Analysis Center, ORNL/Cdiac-145, Oak Ridge National Laboratory, Oak Ridge, Tenessee. NOAA, Pacific Marine Environment (2005); https://www.ncei.noaa.gov/products/ocean-carbon-acidification-data-system.
82. E. Alves, K. Macario, R. Souza, A. Pimenta, K. Douka, F. Oliveira, I. Chanca, R. Angulo, Radiocarbon reservoir corrections on the Brazilian coast from pre-bomb marine shells. *Quat. Geochronol.* **29**, 30–35 (2015).
83. B. Huang, V. F. Banzon, E. Freeman, J. Lavrimore, W. Liu, T. C. Peterson, T. M. Smith, P. W. Thorne, S. D. Woodruff, H.-M. Zhang, Extended reconstructed sea surface temperature version 4 (ERSST.v4). Part I: Upgrades and intercomparisons. *J. Climate* **28**, 911–930 (2015).
84. B. Huang, P. W. Thorne, V. F. Banzon, T. Boyer, G. Chepurin, J. Lavrimore, M. J. Menne, T. M. Smith, R. S. Vose, H.-M. Z hang, Extended reconstructed sea surface temperature, version 5 (ERSSTv5): Upgrades, validations, and intercomparisons. *J. Climate* **30**, 8179–8205 (2017).
85. S. Hetzinger, M. Pfeiffer, W. C. Dullo, E. Ruprecht, D. Garbe-Schönberg, Sr/Ca and $\delta^{18}O$ in a fast-growing *Diploria strigosa* coral: Evaluation of a new climate archive for the tropical Atlantic. *Geochem. Geophys. Geosyst.* **7**, Q10002 (2006).
86. S. Hetzinger, M. Pfeiffer, W. C. Dullo, E. Ruprecht, D. Garbe-Schönberg, J. Halfar, Rapid 20th century warming in the Caribbean and impact of remote forcing on climate in the northern tropical Atlantic as recorded in a Guadeloupe coral. *Paleoceanography* **296**, 111–124 (2010).
87. K. H. Kilbourne, T. M. Quinn, R. Webb, T. Guilderson, J. Nyberg, A. Winter, Paleoclimate proxy perspective on Caribbean climate since the year 1751: Evidence of cooler temperatures and multidecadal variability. *Paleoceanography* **23**, PA3220 (2008).
88. D. Roemmich, The balance of geostrophic and Ekman transports in the tropical Atlantic Ocean. *J. Phys. Oceanogr.* **13**, 1534–1539 (1983).

Acknowledgments: We thank S. Rühs for providing the model-based data of the NBC transport. Helpful discussions with G. Reverdin, E. Michel, C. Hatté and F. Bréon are thanked. **Funding:** This work received the financial support of the CEA-CNRS-UVSQ and the French INSU (Lefe & ST) and ANR-Carquakes programs. **Author contributions:** MP studied and first drafted the design and first wrote the manuscript. E.R.M.D. and T.P.G. wrote the manuscript. D.B. and C. M. did the instrumental data. J.W.-A. and N.F. investigated the corals. **Competing interests:** The authors declare that they have no competing interests **Data and materials availability:** All data needed to evaluate the conclusions in the paper are present in the paper and/or the Supplementary Materials.

Submitted 7 April 2023
Accepted 16 November 2023
Published 15 December 2023
10.1126/sciadv.adi1687